

Submitted: 02/02/2024

Accepted: 22/04/2024

Published: 31/05/2024

Generation and characterization of mesenchymal stem cells from the affected femoral heads of dogs with Legg Calvé Perthes disease

Hinano Eto , Atsushi Yamazaki , Yuma Tomo , Koji Tanegashima 
and Kazuya Edamura* 

Laboratory of Veterinary Surgery, Department of Veterinary Medicine, College of Bioresource and Sciences, Nihon University, Fujisawa, Japan

Abstract

Background: Canine Legg Calvé Perthes disease (LCPD) occurs during the growth period, and the cause of ischemic necrosis of the femoral head during growth remains unclear. If LCPD-affected femoral head-derived mesenchymal stem cells (LCPD-MSCs) can be generated, they can be used as a new tool for the pathophysiological analysis of canine LCPD.

Aim: To generate affected femoral head-derived mesenchymal stem cells (MSCs) from dogs with LCPD and investigate the mRNA expression levels of angiogenesis-related factors and osteogenic differentiation potency of LCPD-MSCs.

Methods: This study was performed using affected femoral heads from dogs diagnosed with LCPD and underwent femoral head and neck ostectomy. The necrotic tissue was harvested from the LCPD-affected femoral head and cultured statically (LCPD group, $n = 6$). Canine bone marrow-derived MSCs (BM-MSCs) were used as controls (control group, $n = 6$). First, the morphology of the cultured cells was observed, and the expression of CD29, CD34, CD44, CD45, CD90, and major histocompatibility complex class II was analyzed using flow cytometry. Additionally, the trilineage differentiation potency of the LCPD-affected head-derived adherent cells was examined. Furthermore, the expression levels of *HIF1A*, *VEGFA*, *VEGFB*, and *PDGFB* mRNAs and the bone differentiation potency of LCPD-affected head-derived adherent cells were investigated.

Results: LCPD-affected femoral head-derived adherent cells showed a fibroblast-like morphology, and the expression of cell surface antigens was similar to that of BM-MSCs. In addition, LCPD-affected femoral head-derived adherent cells showed the same trilineage differentiation potency as BM-MSCs and were consistent with MSC characteristics. Furthermore, the mRNA expression levels of angiogenesis-related factors could be objectively measured in LCPD-MSCs and those MSCs had bone differentiation potency.

Conclusion: In the present study, canine LCPD-MSCs were successfully generated, suggesting their usefulness as a tool for pathological analysis of LCPD in dogs.

Keywords: Angiogenesis related gene, Bone differentiation potency, Dog, Legg Calvé Perthes disease, Mesenchymal stem cell.

Introduction

Legg Calvé Perthes disease (LCPD) is defined as ischemic and aseptic necrosis of the femoral head that occurs during the growth period (Aguado and Goyenvalle, 2021) and was first reported in humans in 1910 (Perthes, 1910) and in dogs by Tutt (1935). Canine LCPD occurs predominantly in certain breeds, such as the Poodle, Yorkshire Terrier, and West Highland Terrier (Pidduck and Webbon, 1978; Boge *et al.*, 2019), and hereditary factors have been reported in the Manchester Terrier (Vasseur *et al.*, 1989). The etiology of canine LCPD includes anatomical abnormalities, susceptibility to intracapsular tamponade, vascular embolism, coagulopathy, and excessive sex hormones

(Rokkanen *et al.*, 1967; Bassett *et al.*, 1969; Aguado and Goyenvalle, 2021). However, the cause of ischemic necrosis of the unilateral femoral head in dogs during growth remains unclear. In our preliminary pathological study using LCPD-affected femoral heads in dogs, ischemic necrosis was observed in all cases. In addition, a preliminary study revealed no infarcts or reconstructive processes by the osteoblasts. Furthermore, immunohistochemical examination of the expression of connective tissue growth factor and vascular endothelial growth factor (VEGF) showed no decrease in the expression of these factors, and the cause of the lack of vascular induction and reduced blood flow to the femoral head could not be determined. Based on this, it is desirable to establish a new pathological

*Corresponding Author: Kazuya Edamura. Laboratory of Veterinary Surgery, Department of Veterinary Medicine, College of Bioresource and Sciences, Nihon University, Fujisawa, Japan. Email: edamura.kazuya@nihon-u.ac.jp

Articles published in Open Veterinary Journal are licensed under a Creative Commons Attribution-NonCommercial 4.0 International License



analysis method to investigate the induction of blood vessels to the femoral head and the bone reconstruction potency in the necrotic area.

In humans, disease-specific induced pluripotent stem cells (iPS cells) generated from patients have been used as a new approach to elucidate the pathogenesis of genetic diseases related to the bone formation by inducing differentiation of mesenchymal stem cells (MSCs) into bone-lineage cells (Mungenast *et al.*, 2016). This stem cell-based approach can be used to analyze the pathophysiology of LCPD and is expected to provide useful information for simulating the condition *in vivo*.

Although there have been some reports on the generation of canine iPS cells (Yoshimatsu *et al.*, 2021, 2022), no disease-specific iPS cells have been generated. In addition, generating pluripotent stem cells is not easy in dogs. Femoral head and neck ostectomy (FHNO) is commonly performed as a surgical treatment for LCPD in dogs, in which the affected femoral head can be obtained directly. If LCPD-affected femoral head-derived MSCs (LCPD-MSCs) can be generated, they are possible to easily analyze the vascular induction and osteogenic potential of stem cells in immature femoral heads. Thus, LCPD-MSCs have the potential to be used as a tool for the pathophysiological analysis of canine LCPD without generating disease-specific iPS cells. However, to the best of our knowledge, there are no reports on the use of such a strategy to analyze the pathogenesis of LCPD.

The objectives of this study were to generate canine LCPD-MSCs, investigate the mRNA expression levels of angiogenesis-related factors and the osteogenic differentiation potential of LCPD-MSCs, and evaluate their usefulness as a tool for the pathophysiological analysis of canine LCPD.

Materials and Methods

Sample collection

This study was performed using the affected femoral heads of dogs diagnosed with LCPD and undergoing FHNO based on clinical signs, palpation, orthopedic examination, and radiographic or CT imaging.

Generation of canine LCPD-affected femoral head-derived MSCs

First, the extracted femoral head was divided through the center of the necrotic area by using an electric surgical blade (Fig. 1A and B). Next, the tissues were harvested from the necrotic area using a small bone curette (Fig. 1C) and placed aseptically in a 6-well plate (Fig. 1D). Harvested tissues were immersed in 0.1 ml of phosphate-buffered saline and transported from the operating room to the culture room. These tissues were then cultured statically in 1.0 ml of alpha modification eagle minimum essential medium (α MEM; Thermo Fisher Scientific Inc., Waltham, MA) supplemented with 10% fetal bovine serum (FBS; Biological Industries, Beit-Haemek, Israel) and 1% penicillin/

streptomycin (Biological Industries) at 5% CO₂ and 37°C. Non-adherent cells were removed by changing the medium every 3–4 days. Once sufficient adherent cells were obtained, the tissues harvested from the affected femoral heads were removed, and cultivation was continued with the same culture medium. When the adherent cells reached 80% confluence, they were collected using 0.25% trypsin-EDTA (Thermo Fisher Scientific Inc.). The collected cells were passaged by seeding at 3.5×10^3 cells/cm² into 75 cm² culture flasks (Thermo Fisher Scientific Inc.) (LCPD group). Bone marrow-derived MSCs (BM-MSCs) from healthy dogs cryopreserved in our laboratory were used as control (control group). In both groups, the morphology of the cultured cells was observed over time under an inverted microscope, and second-passage cells were used for subsequent studies.

Flow cytometry

The cells obtained from one dog were divided into two samples, and six samples from three dogs were used in this study (LCPD group, $n = 6$; control group, $n = 6$). The 3.0×10^5 of the second passaged cells were dispensed into 1.5 ml tubes and then centrifuged at $200 \times g$ for 5 minutes at 4°C to remove the culture medium. Next, the cells were washed twice by adding stain buffer (Becton Dickinson Biosciences, Franklin Lakes, NJ) and centrifuging at $200 \times g$ for 5 minutes at 4°C. To investigate the expression of CD29, CD34, CD44, CD45, CD90, and major histocompatibility complex class II (MHC II), an anti-human CD29 mouse monoclonal antibody (FITC conjugated, Clone No. TS2/16, Thermo Fisher Scientific), anti-canine CD34 mouse monoclonal antibody (FITC-conjugated, Clone No. 1H6, R&D Systems Inc., Minneapolis, MN), and anti-human and -mouse CD44 rat monoclonal antibody (FITC conjugated, Clone No. IM7, Thermo Fisher Scientific), anti-rabbit CD45 rabbit polyclonal antibody (FITC-conjugated, Clone No. RM1007, Abcam UK, Cambridge, UK), anti-canine CD90 rat monoclonal antibody (PE-conjugated, Clone No. YKIX337.217, Thermo Fisher Scientific), and anti-canine MHC class II rat monoclonal antibody (FITC-conjugated, Clone No. YKIX334.2, Thermo Fisher Scientific) were used in this study. These antibodies have been shown to cross dogs (Russell *et al.*, 2016). In both groups, cells in each tube were mixed with primary antibody and incubated at 4°C for 1 hour in the dark. After washing those cells twice with stain buffer, the cell suspensions were filtered through a 35 μ m nylon mesh (Round Bottom Polystyrene Test Tube with Cell Strainer Snap Cap, Becton Dickinson Biosciences). The obtained cells were resuspended in stain buffer and used for flow cytometry. A flow cytometer (BD FACSCanto™ II, Becton Dickinson Biosciences) was used to investigate the expression of cell surface antigens. After removing unstained cells, a minimum of 20,000 events were counted for each analysis. The data obtained were analyzed using dedicated software

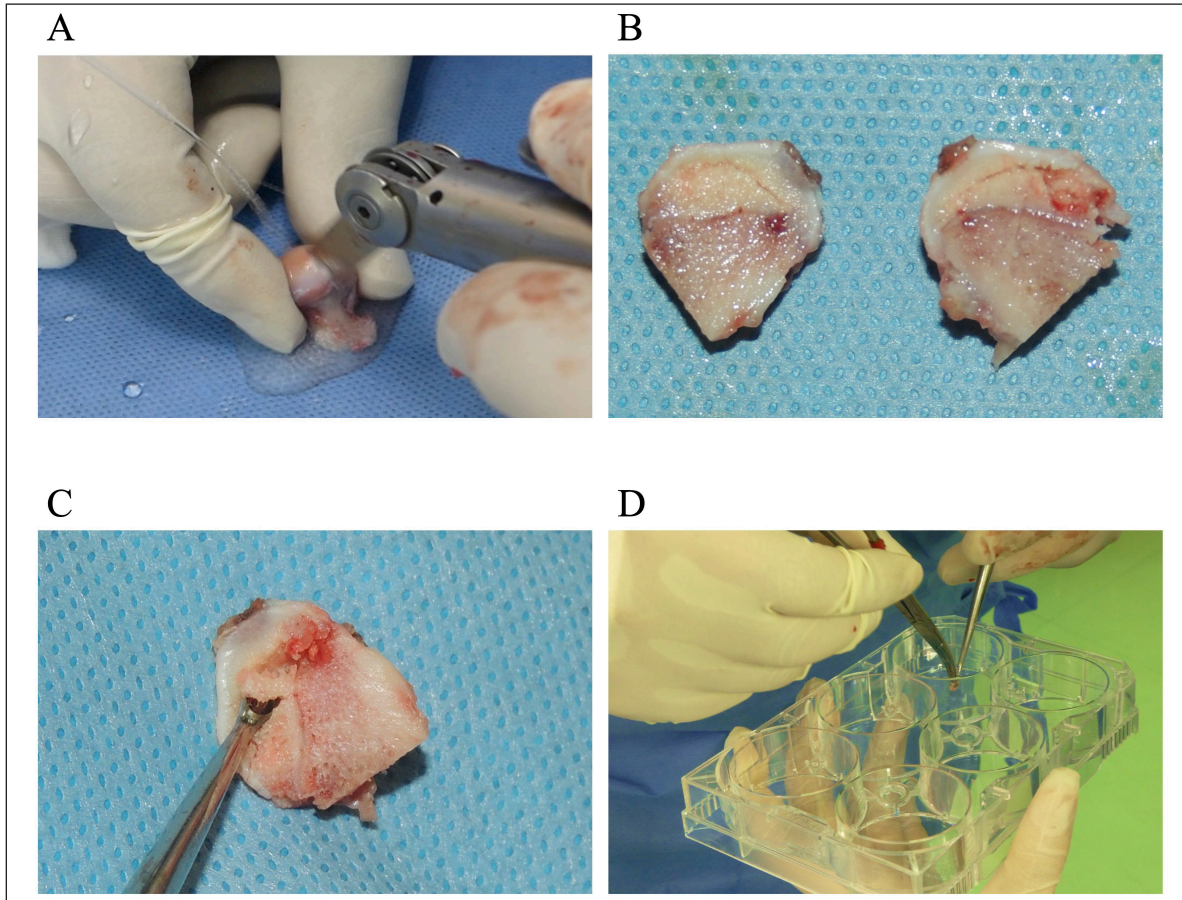


Fig. 1. Harvesting and culturing methods of necrotic tissue from LCPD-affected femoral head. A: Extracted LCPD-affected femoral head was divided through the center of the necrotic area using an electric surgical blade, B: Divided LCPD-affected femoral head, C: Necrotic tissue was harvested with a small bone curette, and D: Aseptic placement of harvested necrotic tissue on a 6-well plate.

(BD FACS Diva™ Version 8.0.1, Becton Dickinson Biosciences). Furthermore, based on previous reports (Takemitsu *et al.*, 2012), the expression of each cell surface marker was classified as “++” if the expression rate was $\geq 70\%$, “+” if the expression rate was between 9% and 69%, and “-” if the expression rate was $< 9\%$, and compared with both groups.

Cell differentiation assay

To evaluate the potential of the obtained cells to differentiate into the mesenchymal cell lineage, their differentiation into adipocytes, osteoblasts, and chondrocytes was induced. In both the LCPD group ($n = 6$) and the control group ($n = 6$), the same second-passaged cells were seeded in 6-well plates at 1.5×10^3 cells/well and cultured with α MEM medium containing 10% FBS until 80% confluency. The culture medium was then changed to a canine adipocyte differentiation medium (Cell Applications, Inc., San Diego, CA), and differentiation into adipocytes was induced by static culture for 3 weeks. Canine osteoblast differentiation medium (Cell Applications, Inc.) was used for

osteoblast differentiation, and the same static culture was performed for 2 weeks. To induce differentiation into chondrocytes, 5×10^5 cells were placed in 15 ml polypropylene tubes, centrifuged to form pellets, and cultured with canine chondrocyte differentiation medium (Cell Applications, Inc.) for 3 weeks. Subsequently, changes in the morphology of cells and cell clusters were observed.

After the induction of differentiation into adipocytes or osteoblasts, adherent cells were fixed with a 4% paraformaldehyde phosphate buffer solution (FUJIFILM Wako Pure Chemical Corporation, Osaka, Japan). After differentiation into chondrocytes, the obtained cell clusters were fixed in methanol. Sudan III, Alizarin Red S, and Alcian Blue staining were performed to confirm the differentiation into adipocytes, osteoblasts, and chondrocytes, respectively.

mRNA expressions of angiogenesis-related factors in LCPD-affected femoral head-derived adherent cells

The second passaged LCPD-affected femoral head-derived adherent cells were seeded in 6-well plates at

Table 1. Canine-specific primers of angiogenesis and osteogenesis-related genes.

Name	Gene symbol	NCBI accession number	Forward primers (5' - 3')	Reverse primers (5' - 3')
GAPDH	<i>GAPDH</i>	NM_001003142.2	GATGGGCGTGAACCATGAGA	AGTGGTCATGGATGACTTTGGCTA
HIF1A	<i>HIF1A</i>	NM_001287163.1	ATGCAAGTCTAGTGAACAGAATGGA	AGGTTTCTGCTGCCTTGTATAGGA
VEGFA	<i>VEGFA</i>	NM_001003175.2	TCAGGACACTGCTGTACTTTGAGG	GGCTTGTGTCAGGAGCAAAGTGAA
VEGFB	<i>VEGFB</i>	XM_038425185	TTCAGACTCAGCAGGGCCACTA	CATGCCGAGGTCTTGGGACTA
PDGFB	<i>PDGFB</i>	XM_038678766.1	TACGAGATGCTGAGCGACCAC	ATCGGGTCAAATTCAGGTCCAA
RUNX2	<i>RUNX2</i>	XM_022425793.1	GCAAAGCCAAATTGCACCA	GGCCTTGGGTAAGGCAAATTC
ALPL	<i>ALPL</i>	NM_001197137.1	CTTAACATGCATTGCCCACTCC	TGACCACAAAGACTCAGTTCTGTCC
SPP1	<i>SPP1</i>	XM_003434024.4	TTCCCACTGACATTCCAGCAAC	GGACCTCAGTCCATAAGCCACAC
ALPL	<i>ALPL</i>	NM_001197137.1	CTTAACATGCATTGCCCACTCC	TGACCACAAAGACTCAGTTCTGTCC

1.5×10^3 cells/well and cultured with α MEM containing 10% FBS until 80% confluency to investigate the expressions of angiogenesis-related genes ($n = 6$). Adherent cells were collected using 1 ml of Buffer RLT (QIAGEN, Venlo, Netherlands) and agitated using a vortex mixer (Scientific Industries, Bohemia, NY). Total RNA was extracted using the method described below and used for qPCR. In this study, the expression levels of *HIF1A*, *VEGFA*, *VEGFB*, and *PDGFB* mRNA were analyzed as angiogenesis-related genes.

Osteogenic potency of LCPD-affected femoral head-derived adherent cells

The second passaged LCPD-affected femoral head-derived adherent cells were seeded in 6-well plates at 1.5×10^3 cells/well and cultured with α MEM containing 10% FBS until 80% confluency to determine the osteogenic potency ($n = 6$). The culture medium was then changed to canine osteoblast differentiation medium (Cell Applications, Inc.) as described above to differentiate the LCPD-affected femoral head-derived adherent cells into osteoblasts. After 1 week of differentiation into osteoblasts, adherent cells were collected in Buffer RLT and agitated using a vortex. Total RNA was extracted using the method described below and was used for qPCR. In this study, the expression levels of runt-related transcription factor 2 (*RUNX2*), alkaline phosphatase (*ALPL*), and secreted phosphoprotein 1 (*SPP1*) mRNA were compared before and after osteoblast differentiation to investigate their osteogenic potency.

mRNA expression analysis using quantitative real-time PCR

Total RNA was extracted using the RNeasy Mini Kit (QIAGEN), and cDNA was then synthesized from 125–1,000 ng of total RNA using Prime Script RT Master Mix (TaKaRa Bio Inc., Shiga, Japan) and My Genie 32 Thermal Block (BINEER Co., Daejeon, Korea). Quantitative real-time PCR (RT-qPCR) was performed using 6.25 ng of template cDNA, TB Green Premix Ex Taq II (TaKaRa Bio Inc.), and canine-specific primer sets (Table 1). PCR reactions were performed using the

Thermal Cycler Dice1 Real Time System II (TaKaRa Bio Inc.) with an initial denaturation at 95°C for 30 seconds followed by 40 cycles of denaturation at 95°C for 5 seconds, annealing and extension at 60°C for 30 seconds. Finally, a dissociation curve analysis was performed to confirm the specificity of the PCR.

The results obtained by RT-qPCR were analyzed by the comparative cycle threshold (Δ Ct) method using TP900 DiceRealTime v4.02B (TaKaRa Bio Inc.). The expression level of each gene was calculated using the relative expression level of *GAPDH* as the housekeeping gene.

Statistical analysis

The data obtained from the described experiments were calculated as mean \pm standard deviation. Statistical analysis was performed using statistical software (GraphPad Prism version 6.0, Macintosh, GraphPad Software Inc., Boston, MA), and The Mann–Whitney *U* test was used to compare the two groups. Statistical significance was set at $p < 0.05$.

Ethical approval

This study was approved by the Clinical Research and Trial Ethics Committee of the Animal Medical Center of Nihon University (ANMEC-3-027). Consent to use the samples collected for this study was obtained from all dog owners.

Results

Morphology of canine LCPD-affected femoral head-derived adherent cells

When the tissues harvested from LCPD-affected femoral heads were cultured statically, spindle-shaped, fibroblast-like adherent cells were obtained after approximately 7 days of culture, and their morphologies were similar to those of BM-MSCs (Fig. 2A). These adherent cells proliferated outward, centered on the static tissue (Fig. 2B), and became 80% confluent after approximately 14 days of culture (Fig. 2C). Adherent cells maintained their fibroblast-like morphology and expanded vigorously even after passage.

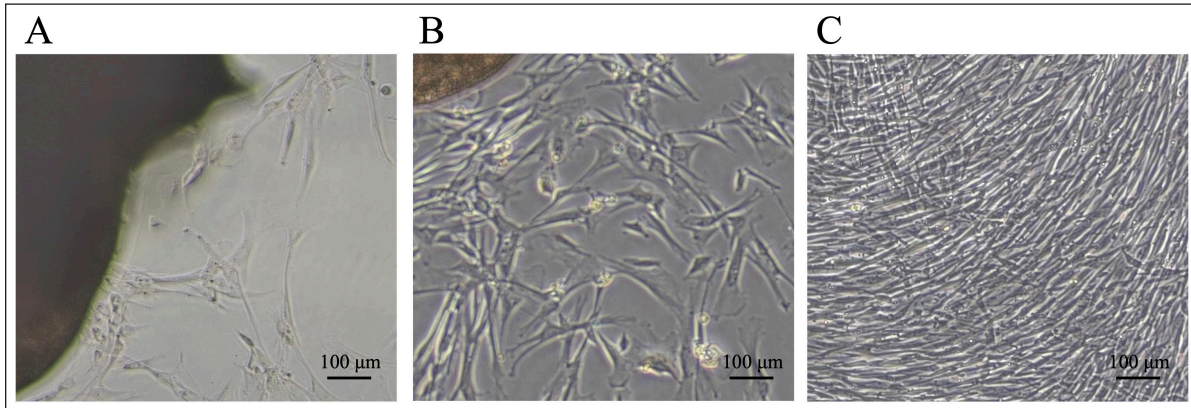


Fig. 2. Morphologies of canine LCPD-affected femoral head-derived adherent cells. A: Day 7, B: Day 10, C: Day 14, Scale bars, 100 µm.

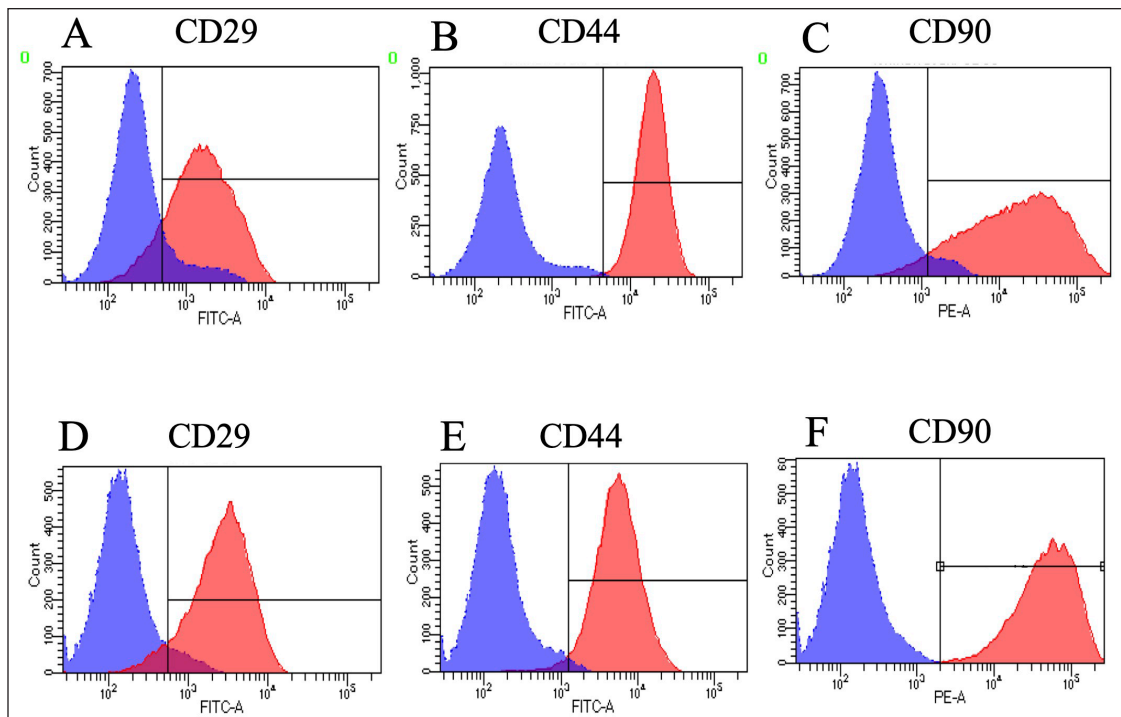


Fig. 3. Expressions of cell surface antigens as positive marker in canine BM-MSCs and LCPD-affected femoral head-derived adherent cells. Flow cytometry analysis revealed that canine BM-MSCs (A–C) and LCPD-affected femoral head-derived adherent cells (D–F) expressed CD29 (A and D), CD44 (B and E), and CD90 (C and F). Blue area: negative isotype control; Red area: samples.

Expressions of cell surface antigens

When the expression of surface antigens on cells in the LCPD and control groups was compared using flow cytometry, the CD29, CD44, and CD90 expression levels were similar in both groups (Fig. 3). In the LCPD group, the expression rates of CD29, CD44, and CD90 were $77.9 \pm 5.5\%$ (++) , $79.5 \pm 10.4\%$ (++) , and $77.6 \pm 12.1\%$ (++) , respectively. In the control group, the expression rates of CD29, CD44, and CD90 were 73.4

$\pm 9.5\%$ (++) , $85.9 \pm 5.1\%$ (++) , and $81.3 \pm 3.8\%$ (++) , respectively. By contrast, CD34, CD45, and MHC II were rarely expressed in either group (Fig. 4). In the LCPD group, the expression rates of CD34, CD45, and MHC class II were $1.5 \pm 1.3\%$ (-) , 3.0 ± 2.0 (-) , and $1.1 \pm 0.9\%$ (-) , respectively. In the control group, the expression rates of CD34, CD45, and MHC class II were $6.4 \pm 4.3\%$ (-) , 6.8 ± 4.8 (-) , and $6.3 \pm 3.8\%$ (-) , respectively. Accordingly, the expression patterns of

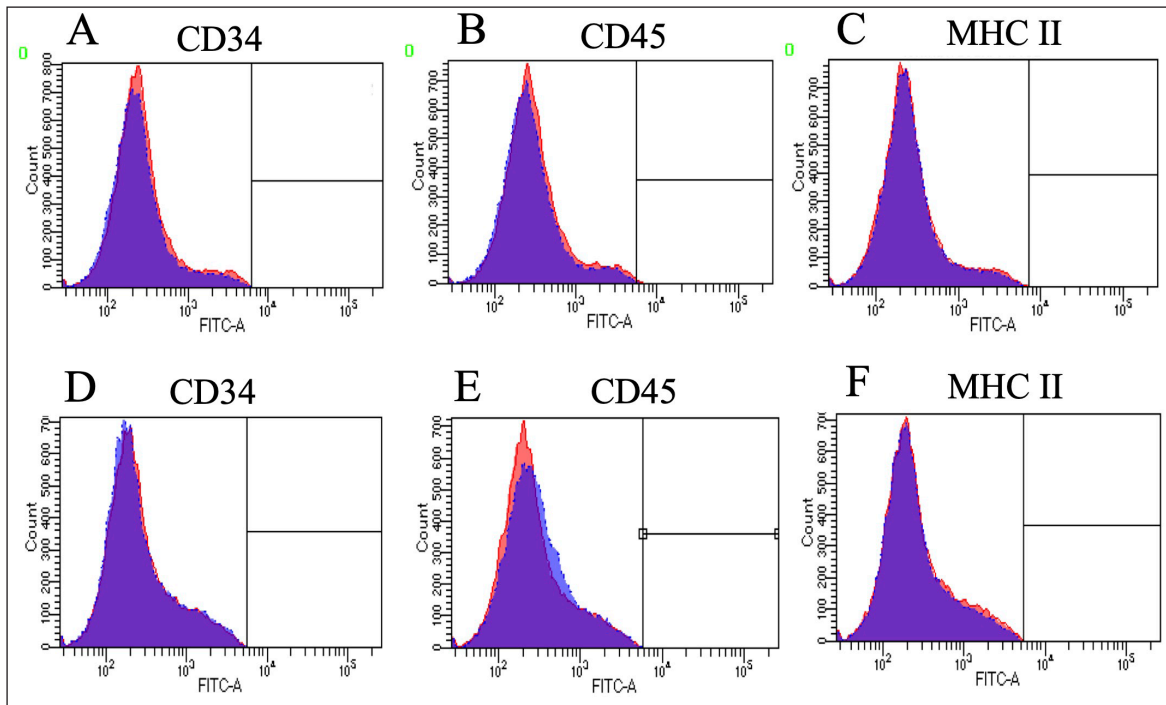


Fig. 4. Expressions of cell surface antigens as negative marker in canine BM-MSCs and LCPD-affected femoral head-derived adherent cells. Flow cytometry analysis revealed that canine BM-MSCs (A–C) and LCPD-affected femoral head-derived adherent cells (D–F) lacked expression of CD34 (A and D), CD45 (B and E), and MHC class II (C and F) expression. Blue area: negative isotype control; red area: samples.

Table 2. Expression of cell surface antigens.

	CD29	CD34	CD44	CD45	CD90	MHC II
Control	++	–	++	–	++	–
LCPD	++	–	++	–	++	–

Samples were scored as “–” if <9% of cells were positive, “+” if 9%–69% were positive, and “++” if ≥70% were positive.

cell surface antigens in LCPD-affected femoral head-derived adherent cells and BM-MSCs obtained in this study were identical (Table 2).

Trilineage cell differentiation

After inducing the differentiation of LCPD-affected femoral head-derived adherent cells into adipocytes, their morphology changed after approximately 7 days, and lipid droplet-like structures appeared in the cytoplasm after approximately 10 days. Three weeks after the induction of adipocyte differentiation, the lipid droplet-like structures in the cells were stained reddish-orange by Zudan III staining, indicating that they differentiated into adipocytes (Fig. 5A).

When LCPD-affected femoral head-derived adherent cells differentiated into osteoblasts, the cells began to aggregate after approximately 5 days and formed colony-like cell aggregates after approximately 10 days. Alizarin red staining of the cells obtained 2 weeks after the induction of osteoblast differentiation showed

that the cell aggregates were dark red, indicating that the cells differentiated into osteoblasts (Fig. 5B).

When LCPD-affected femoral head-derived adherent cells were differentiated into chondrocytes using the pellet culture method, white spherical cell clusters were formed after approximately 14 days. Alcian blue staining of the cell cluster after 3 weeks of induced differentiation into chondrocytes showed that the cluster was stained blue, indicating that the cells had differentiated into chondrocytes (Fig. 5C). Accordingly, LCPD-affected femoral head-derived adherent cells had the same trilineage differentiation potency as BM-MSCs (Fig. 5D–F) and were consistent with MSC characteristics.

mRNA expressions of angiogenesis-related factors in LCPD-MSCs

When the expression of angiogenesis-related genes in LCPD-MSCs was analyzed by qPCR, *HIF1A*, *VEGFA*,

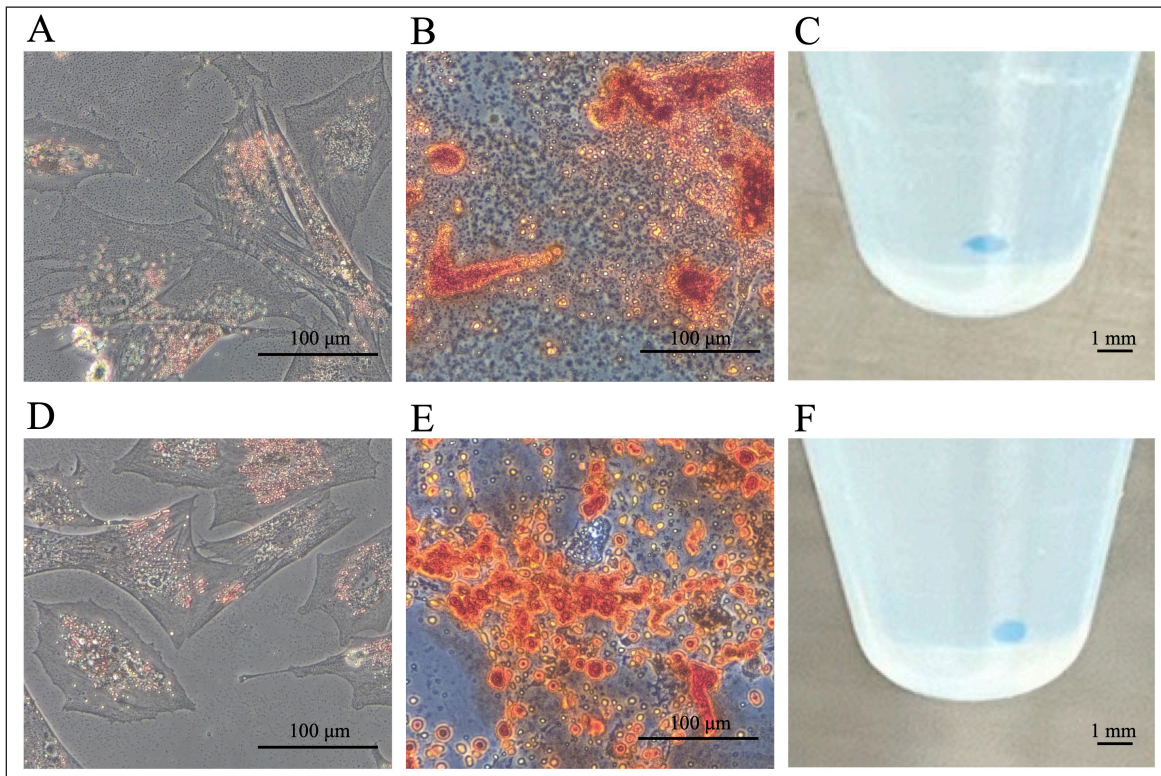


Fig. 5. Trilineage differentiation potency. Canine LCPD-affected femoral head-derived adherent cells (A-C) and BM-MSCs (D-F) differentiated into adipocytes (A and D), osteoblasts (B and E), and chondrocytes (C and F). (A and D): Sudan III staining, (B and E): Alizarin Red staining, and (C and F): Alcian blue staining. Scale bars = 100 μ m or 1 mm.

Table 3. Relative expressions of angiogenesis-related genes.

Gene name	<i>HIF1A</i>	<i>VEGFA</i>	<i>VEGFB</i>	<i>PDGFB</i>
Relative expression	0.089 \pm 0.036	0.054 \pm 0.012	0.030 \pm 0.011	0.000014 \pm 0.0000057

VEGFB, and *PDGFB* mRNA expression was observed, all of which could be quantified (Table 3).

Osteogenic potency of LCPD-MSCs

A comparison of the expression levels of mRNA related to bone formation before and after the differentiation of LCPD-MSCs into osteoblasts revealed a significant increase in the expression level of *SPP1* mRNA. The expression levels of *RUNX2* and *ALPL* mRNAs also tended to increase after differentiation into osteoblasts (Fig. 6).

Discussion

Canine LCPD causes ischemic necrosis of the femoral head during growth, and the necrotic area does not regenerate and progresses irreversibly. Although several histopathological studies focused on vascular induction factors, such as HIF-1 α and VEGF as causes of femoral head ischemia (Liu *et al.*, 2012; Zhang *et al.*, 2012), the factors involved in this pathophysiology have not yet been identified. Therefore, in this study, we hypothesized that vascular induction factors

derived from stem cells in the femoral head affect the pathogenesis of LCPD in dogs and attempted to isolate MSCs from the LCPD-affected femoral head to investigate the expression of angiogenesis-related genes. In addition, as mentioned above, bone reconstruction by osteoblasts was not observed in the LCPD-affected femoral heads, contributing to the progression of this disease. However, to the best of our knowledge, the osteogenic potency of MSCs in LCPD-affected femoral heads has not yet been investigated. Therefore, the present study examined the osteogenic potency of MSCs derived from LCPD-affected femoral heads. These investigations differ from previously reported histopathological studies as they were examined using live cells, which is expected to provide new knowledge.

MSCs are characterized by their fibroblast-like morphology and ability to adhere to plastics under standard culture conditions (Dominici *et al.*, 2006). MSCs also express specific cell surface antigens and exhibit multipotent differentiation into adipocytes,

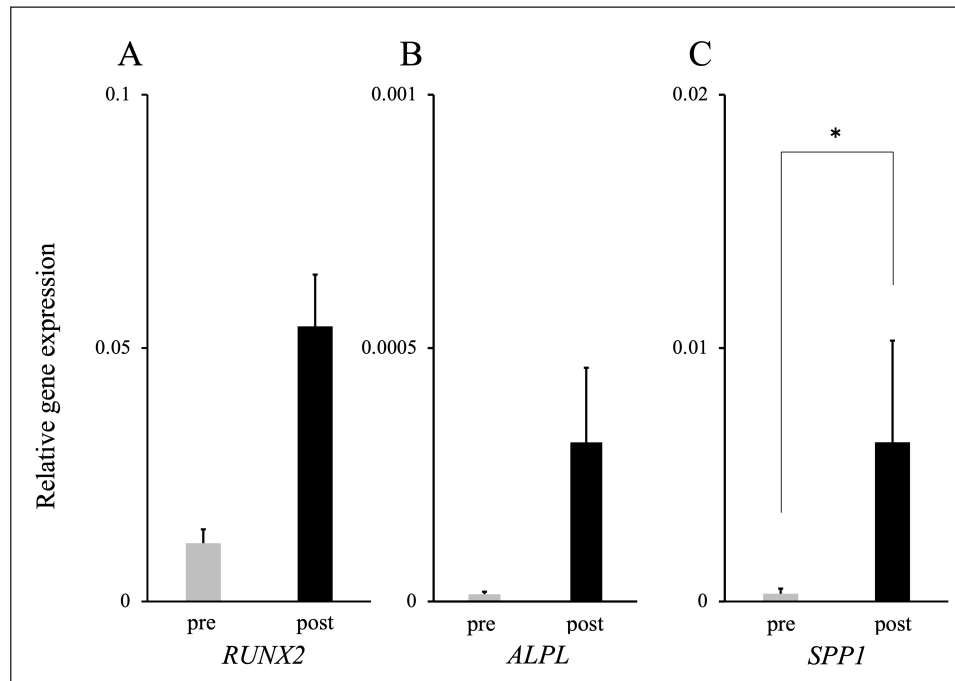


Fig. 6. mRNA expression levels after bone differentiation of LCPD-MSCs. The expressions of *RUNX2*, *ALPL*, and *SPP1* mRNAs increased after bone differentiation. A: *RUNX2*, B: *ALPL*, and C: *SPP1*. The data are presented as mean \pm standard deviation. *: Significant difference between the two groups ($p < 0.05$).

osteoblasts, and chondrocytes (Dominici *et al.*, 2006). Plastic adherent cells isolated from the LCPD-affected femoral head showed a fibroblast-like morphology, which was very similar to that of canine BM-MSCs (Fig. 2). Human MSCs have been identified to express the cell surface antigens CD73, CD90, and CD105, but not CD11b, CD14, CD19, CD34, CD45, CD79a, or HLA-DR (Dominici *et al.*, 2006). However, the expression of these cell surface antigens differs in canine MSCs and remains under investigation. Several studies have analyzed the expression of specific cell surface antigens in canine MSCs using flow cytometry (Kamishina *et al.*, 2006; Csaki *et al.*, 2007; Kisiel *et al.*, 2012; Reich *et al.*, 2012; Takemitsu *et al.*, 2012; Zhang *et al.*, 2013; Screven *et al.*, 2014). These reports indicate that canine MSCs express CD29, CD44, and CD90, whereas CD34, CD45, and MHC class II are either absent or weakly expressed (Kamishina *et al.*, 2006; Csaki *et al.*, 2007; Kisiel *et al.*, 2012; Reich *et al.*, 2012; Takemitsu *et al.*, 2012; Zhang *et al.*, 2013; Screven *et al.*, 2014). Therefore, in the present study, the expressions of CD29, CD34, CD44, CD45, CD90, and MHC class II in canine LCPD-affected femoral head-derived adherent cells were investigated. The results of the present study were identical to those of previous studies and showed the same trend as the expression of cell surface antigens in BM-MSCs (Figs. 3 and 4). Furthermore, in the present study, canine

LCPD-affected femoral head-derived adherent cells were differentiated into adipocytes, osteoblasts, and chondroblasts using a previously reported method (Takemitsu *et al.*, 2012; Matsuda *et al.*, 2017). LCPD-affected femoral head-derived adherent cells had the same trilineage differentiation potency as canine BM-MSCs (Fig. 5). These results suggested that the LCPD-affected femoral head-derived adherent cells obtained in the present study were MSCs.

In humans, angiogenesis-related factors, such as *HIF1A* and *VEGF mRNAs*, may be involved in the pathogenesis of LCPD (Zhang *et al.*, 2015; Hong *et al.*, 2016; Tiwari *et al.*, 2018). A study using an LCPD rabbit model revealed that *VEGF* mRNA expression was lower in the thickened region of the epiphyseal cartilage after femoral head necrosis (Li *et al.*, 2008). Another study using a rabbit model of femoral head avascular necrosis showed that *PDGFB* mRNA expression levels were significantly lower in the model group than in the control group (Zhang *et al.*, 2018). Therefore, mRNA expression of *HIF1A*, *VEGFA*, *VEGFB*, and *PDGFB* in LCPD-MSCs was investigated in the present study. The expression of all investigated angiogenesis-related genes was objectively confirmed and successfully quantified. Subsequent studies will be performed to generate MSCs derived from the femoral head of normal dogs using the technology established in this study and compare them with LCPD-MSCs to

clarify the angiogenesis-related genes involved in the pathogenesis of LCPD in dogs.

To the best of our knowledge, there have been no reports on the osteogenic potency of LCPD-MSCs in humans or dogs. In the present study, when LCPD-MSCs were induced to differentiate into osteoblasts, the *RUNX2*, *ALPL*, and *SPP1* mRNA expression levels increased. *RUNX2* is an essential transcription factor for the differentiation of MSCs into preosteoblasts (Kawane et al., 2018). It has also been reported that *ALPL* is expressed when MSCs are induced to differentiate into osteoblasts and is widely used as an indicator of osteoblast differentiation (Gousopoulou et al., 2021). *SPP1*, also known as osteopontin, is produced by osteoblasts and osteoclasts and plays an important role in bone formation, resorption, and remodeling (Terai et al., 1999). In the present study, the expression of these mRNAs was upregulated in cells induced to differentiate from LCPD-MSCs. These results suggest that LCPD-MSCs have osteogenic potency.

The greatest limitation of the present study was the small number of investigated cases because this study was performed using affected femoral heads from dogs with spontaneous LCPD. In addition, this study was performed *in vitro* using LCPD-MSCs, which may differ from the *in vivo* pathophysiology. Only dogs with LCPD were included in this study. Therefore, it is necessary to compare LCPD-MSCs with MSCs isolated from femoral heads of healthy dogs to clarify the pathogenesis of canine LCPD.

Conclusion

In this study, MSCs derived from LCPD-affected femoral heads were successfully generated for the first time in dogs. The mRNA expression levels of angiogenesis-related genes were quantified in canine LCPD-MSCs. Furthermore, LCPD-MSCs could differentiate into osteoblasts. Canine LCPD-MSCs generated in this study cannot be used for therapy for LCPD because they are disease-derived MSCs, but they have the potential to contribute to the analysis of LCPD pathogenesis in dogs.

Acknowledgments

None.

Conflicts of interest

The authors declare that there is no conflict of interest.

Funding

No funding was received to assist with the preparation of this manuscript.

Data availability

To access the data, kindly contact the corresponding author.

Authors' contributions

All authors conceived and performed the procedures; drafted, revised the manuscript, and approved the final version of the manuscript.

References

- Aguado, E. and Goyenvalle, E. 2021. Legg Calvé Perthes disease in the dog. *Morphologie* 105, 143–147.
- Bassett, F.H.I., Wilson, J.W., Allen, B.L.J. and Azuma, H. 1969. Normal vascular anatomy of the head of the femur in puppies with emphasis on the inferior reticular vessels. *J. Bone Joint Surg.* 51(6), 1139–1153.
- Boge, G.S., Moldal, E.R., Dimopoulou, M., Skjerve, E. and Bergström, A. 2019. Breed susceptibility for common surgically treated orthopaedic diseases in 12 dog breeds. *Acta Vet. Scand.* 61(1), 19.
- Csaki, C., Matis, U., Mobasheri, A., Ye, H. and Shakibaei, M. 2007. Chondrogenesis, osteogenesis and adipogenesis of canine mesenchymal stem cells: a biochemical, morphological and ultrastructural study. *Histochem. Cell Biol.* 128(6), 507–520.
- Dominici, M., Le Blanc, K., Mueller, I., Slaper-Cortenbach, I., Marini, F., Krause, D., Deans, R., Keating, A., Prockop, D.J. and Horwitz, E. 2006. Minimal criteria for defining multipotent mesenchymal stromal cells. The international society for cellular therapy position statement. *Cytotherapy* 8(4), 315–317.
- Gousopoulou, E., Bakopoulou, A., Apatzidou, D.A., Leyhausen, G., Volk, J., Staufenbiel, I., Geurtsen, W. and Adam, K. 2021. Evaluation of stemness properties of cells derived from granulation tissue of peri-implantitis lesions. *Clin. Exp. Dent. Res.* 7(5), 739–753.
- Hong, G.J., Lin, N., Chen, L.L., Chen, X.B. and He, W. 2016. Association between vascular endothelial growth factor gene polymorphisms and the risk of osteonecrosis of the femoral head: systematic review. *Biomed. Rep.* 4(1), 92–96.
- Kamishina, H., Deng, J., Oji, T., Cheeseman, J.A. and Clemmons, R.M. 2006. Expression of neural markers on bone marrow-derived canine mesenchymal stem cells. *Am. J. Vet. Res.* 67(11), 1921–1928.
- Kawane, T., Qin, X., Jiang, Q., Miyazaki, T., Komori, H., Yoshida, C.A., Matsuura-Kawata, V.K.D.S., Sakane, C., Matsuo, Y., Nagai, K., Maeno, T., Date, Y., Nishimura, R. and Komori, T. 2018. Runx2 is required for the proliferation of osteoblast progenitors and induces proliferation by regulating *Fgfr2* and *Fgfr3*. *Sci. Rep.* 8(1), 13551.
- Kisiel, A.H., McDuffee, L.A., Masaoud, E., Bailey, T.R., Gonzalez, B.P.E. and Nino-Fong, R. 2012. Isolation, characterization, and *in vitro* proliferation of canine mesenchymal stem cells derived from bone marrow, adipose tissue, muscle, and periosteum. *Am. J. Vet. Res.* 73(8), 1305–1317.
- Li, W., Fan, Q., Ma, B., Ren, M., Li, H., Gou, Y. and Qian, J. 2008. An animal model of Perthes disease and an experimental research of VEGF expression.

- Zhongguo Xiu Fu Chong Jian Wai Ke Za Zhi. 22(7), 814–819.
- Liu, C., Zhao, D. and Wang, B. 2012. Effects of different stress force stimulations on the expression of vascular endothelial growth factor in Beagle dogs in the repairing process of osteonecrosis of the femoral head. *Zhonghua Yi Xue Za Zhi* 92(1), 40–44.
- Matsuda, T., Takami, T., Sasaki, R., Nishimura, T., Aibe, Y., Paredes, B.D., Quintanilha, L.F., Matsumoto, T., Ishikawa, T., Yamamoto, N., Tani, K., Terai, S., Taura, Y. and Sakaida I. 2017. A canine liver fibrosis model to develop a therapy for liver cirrhosis using cultured bone marrow-derived cells. *Hepatology* 1(7), 691–703.
- Mungenast, A.E., Siegert, S. and Tsai, L.H. 2016. Modeling Alzheimer's disease with human induced pluripotent stem (iPS) cells. *Mol. Cell Neurosci.* 73, 13–31.
- Perthes, G. 1910. Über Arthritis deformans juvenilis. *Deutsche Zeitschrift für Chirurgie* 107, 111–159.
- Pidduck, H. and Webbon, P.M. 1978. The genetic control of Perthes' disease in toy poodles—a working hypothesis. *J. Small Anim. Pract.* 19(12), 729–733.
- Reich, C.M., Raabe, O., Wensch, S., Bridger, P.S., Kramer, M. and Arnhold, S. 2012. Isolation, culture and chondrogenic differentiation of canine adipose tissue- and bone marrow-derived mesenchymal stem cells—a comparative study. *Vet. Res. Commun.* 36(2), 139–148.
- Rokkanen, P., Paatsama, S. and Rissanen, P. 1967. Changes in the femoral head induced with certain hormones. An experimental study of young dogs. *Ann. Chir. Gynaecol. Fenn.* 56(4), 456–463.
- Russell, K.A., Chow, N.H.C., Dukoff, D., Gibson, T.W.G., LaMarre, J., Betts, D.H. and Koch, T.G. 2016. Characterization and immunomodulatory effects of canine adipose tissue- and bone marrow-derived mesenchymal stromal cells. *PLoS One* 11(12), e0167442.
- Screven, R., Kenyon, E., Myers, M.J., Yancy, H.F., Skasko, M., Boxer, L., Bigley, E.C. 3rd, Borjesson, D.L. and Zhu, M. 2014. Immunophenotype and gene expression profile of mesenchymal stem cells derived from canine adipose tissue and bone marrow. *Vet. Immunol. Immunopathol.* 161(1-2), 21–31.
- Takemitsu, H., Zhao, D., Yamamoto, I., Harada, Y., Michishita, M. and Arai, T. 2012. Comparison of bone marrow and adipose tissue-derived canine mesenchymal stem cells. *BMC Vet. Res.* 8, 150.
- Terai, K., Takano-Yamamoto, T., Ohba, Y., Hiura, K., Sugimoto, M., Sato, M., Kawahata, H., Inaguma, N., Kitamura, Y. and Nomura, S. 1999. Role of osteopontin in bone remodeling caused by mechanical stress. *J. Bone Miner. Res.* 14(6), 839–849.
- Tiwari, V., Poudel, R.R., Khan, S.A., Mehra, S., Chauhan, S.S. and Rajee, A. 2018. Is VEGF under-expressed in Indian children with Perthes disease? *Musculoskelet. Surg.* 102(1), 81–85.
- Tutt, J. 1935. Tuberculosis of the hip joint in a cairn terrier. *Vet. Rec.* 47, 428–431.
- Vasseur, P.B., Foley, P., Stevenson, S. and Heitter, D. 1989. Mode of inheritance of Perthes' disease in Manchester terriers. *Clin. Orthop. Relat. Res.* 244, 281–292.
- Yoshimatsu, S., Nakajima, M., Iguchi, A., Sanosaka, T., Sato, T., Nakamura, M., Nakajima, R., Arai, E., Ishikawa, M., Imaizumi, K., Watanabe, H., Okahara, J., Noce, T., Takeda, Y., Sasaki, E., Behr, R., Edamura, K., Shiozawa, S. and Okano, H. 2021. Non-viral induction of transgene-free iPSCs from somatic fibroblasts of multiple mammalian species. *Stem Cell Rep.* 16(4), 754–770.
- Yoshimatsu, S., Yamazaki, A., Edamura, K., Koushige, Y., Shibuya, H., Qian, E., Sato, T., Okahara, J., Kishi, N., Noce, T., Yamaguchi, Y. and Okano, H. 2022. Step-by-step protocols for non-viral derivation of transgene-free induced pluripotent stem cells from somatic fibroblasts of multiple mammalian species. *Dev. Growth Differ.* 64(6), 325–341.
- Zhang, N., Dietrich, M.A. and Lopez, M.J. 2013. Canine intra-articular multipotent stromal cells (MSC) from adipose tissue have the highest *in vitro* expansion rates, multipotentiality, and MSC immunophenotypes. *Vet. Surg.* 42(2), 137–146.
- Zhang, C., Li, Y., Cornelia, R., Swisher, S. and Kim, H. 2012. Regulation of VEGF expression by HIF-1 α in the femoral head cartilage following ischemia osteonecrosis. *Sci. Rep.* 2, 650.
- Zhang, X.L., Shi, K.Q., Jia, P.T., Jiang, L.H., Liu, Y.H., Chen, X., Zhou, Z.Y., Li, Y.X. and Wang, L.S. 2018. Effects of platelet-rich plasma on angiogenesis and osteogenesis-associated factors in rabbits with avascular necrosis of the femoral head. *Eur. Rev. Med. Pharmacol. Sci.* 22(7), 2143–2152.
- Zhang, W., Yuan, Z., Pei, X. and Ma, R. 2015. *In vivo* and *in vitro* characteristic of HIF-1 α and relative genes in ischemic femoral head necrosis. *Int. J. Clin. Exp. Pathol.* 8(6), 7210–7216.